

Stability Analysis of Special-Shape Arch Bridge

Wen-Liang Qiu¹, Chin-Sheng Kao^{2*}, Chang-Huan Kou³, Jeng-Lin Tsai³ and Guang Yang¹

¹*School of Civil Engineering, Dalian University of Technology,
Dalian City, Liaoning Province 116024, P.R. China*

²*Department of Civil Engineering, Tamkang University,
Tamsui, Taiwan 251, R.O.C.*

³*Department of Civil Engineering and Engineering Informatics, Chunghua University,
Hsinchu, Taiwan 300, R.O.C.*

Abstract

This paper presents a stability investigation of a special-shape arch bridge with a span of 180 m. Its structure and mechanics are significantly different from normal arch bridges because of its single arch rib skewing across the girder, its hangers hanging unevenly along the arch rib with different aslant angle, and its arch rib being subjected to massive axial compression force, bending moment, torque, and shear stress. In this paper, the eigenvalue method is used to analyze some of the main influencing factors, such as different loads, restraint conditions of arch spring, stiffness of arch rib, stiffness of main girder and rise-span ratio of arch rib. The study results showed that the slant hangers at both sides of the girder reduced the tendency of arch instability, which is obviously helpful to maintain overall structural stability. Increasing the height of the main girder can improve the structural stability, but the effect is limited. The restrained conditions of the arch spring markedly influence the overall structural stability, and the stability coefficient of a fixed arch is more than twice the coefficient of a two-hinge arch. The rise-span ratio has a relatively large impact on the stability coefficient. A reasonable rise-span ratio for the special-shape arch bridge studied here is around 0.37 that is larger than an expected ratio for a normal arch bridge obtained in existed studies. The impacts of vertical flexural stiffness and lateral flexural stiffness of the arch rib on the structural stability are determined by the mode of buckling, and the lateral flexural stiffness has nearly no impact on the structural stability for an in-plane buckling arch.

Key Words: Special-Shape Arch Bridge, Stability, Geometric Nonlinear

1. Introduction

With continuous improvements in the aesthetics of bridges, bridges with traditional and simple designs can no longer satisfy demands of visual appeal. Consequently, some new special-shape arch bridges have gradually been presented to the world.

Special-shape arch bridges differ from normal arch bridges in that, in special-shape arch bridges, arch ribs are configured askew across the main girders, and han-

gers are configured at different angles, thereby creating a unique dynamic effect.

The stability problem is an important issue in the field of mechanics and is a problem often encountered in bridge engineering; the stability problem is of equal importance to the strength problem. The stability problems associated with askew configuration of arch components in special-shape arch bridges is a subject of even greater concern.

Structural stability analysis theory has gradually developed and formed since Euler introduced the Euler Formula for dealing with the buckling of slender struts

*Corresponding author. E-mail: csk@mail.tku.edu.tw

over two centuries ago. Timoshenko and Gere (1961) and Ziegler Hans (1968) have made comprehensive expositions of structural stability theory. Early research on steel arch in-plane buckling mainly employed classical buckling theory [1,2]. Austin and Ross (1976) studied the impact of the rise-span ratio of two-dimensional parabolic arches and circular arches on in-plane buckling loads, and found that the parabolic arches had larger buckling loads than catenary arches and circular arches [3]. In a study on in-plane buckling of parabolic arches, Harrison (1982) found that the buckling load limits of local loads are significantly smaller than overall loads [4]. In researches on in-plane inelastic buckling, Mirmiran and Amde (1993) studied inelastic buckling of prestressed arches [5]. Pi and Trahair (1996) studied the impact of many factors such as arch slenderness ratio, obliquity, initial bending, and residual stress on the in-plane inelastic buckling strength of circular steel arches [6]. Using FEM and considering effects of broken cable, Arie Romeijn and Charalampos Bouras (2008) investigated the in-plane buckling length factor of the arches [7].

In studying the lateral stability of arches, Timoshenko (1961) used an analytical method to resolve the out-of-plane buckling problem of circular arches under uniform radial loads [1]. Stüssi studied the problem of lateral buckling in tied-arches and deck arches, but did not consider the contribution of deck systems in raising buckling loads [8]. Wen and Medallah (1987) performed research on the in-plane and out-of-plane stability of deck arch, and found that the lateral buckling load was markedly affected by the stiffness of deck and the effects depended on the stiffness of arch ribs and bracing system between the ribs [9]. Raymond H. Plaut (1990) employed analytical methods to research the stability of flat arch bridges with both ends elastically restrained and gave the relationship between buckling load and stiffness of the elastic restraint [10]. Considering the effects of structure parameters, such as the flexural rigidity, number and position of crossbeam, rise-to-span of arch ribs and inclination of ribs, Pan S. S. (2004) studied the lateral stability of CFST narrow arch bridge [11]. Xing F. et al. (2009) studied the nonlinear stability of CFST basket handle arch bridge and gave its ultimate bearing capacity [12].

For the special-shape arch bridge studied in this paper, because its single arch rib skews across the girder

and its hangers with different aslant angle are designed unevenly along the arch rib, the arch rib is subject to massive axial compression force as well as large bending moment, torque, and shear stress. These characteristics differ significantly from the structures and mechanics of normal arch bridges, giving the bridge's stability its uniqueness. This paper uses the eigenvalue method to perform detailed study on the stability problem in a special-shape arch bridge, taking into account the impacts of different loads, restraint conditions, stiffness of arch rib, stiffness of deck and rise-span ratio of arch rib.

2. Stability Analysis of Arch Bridge and Non-Directional Force

2.1 In-Plane Buckling of Arch

When the load gradually increases to the critical value, bending deformation will appear in equilibrium process, causing the arch to begin buckling. This is the first type of in-plane buckling of arch.

The second type of buckling is shown in Figure 1. Under asymmetric loads, arches will produce horizontal displacement and vertical displacement. The displacements in two directions will increase with the load increasing. When the load reaches the critical load, displacement increases rapidly. This type of instability is referred to as extreme point instability or Type 2 in-

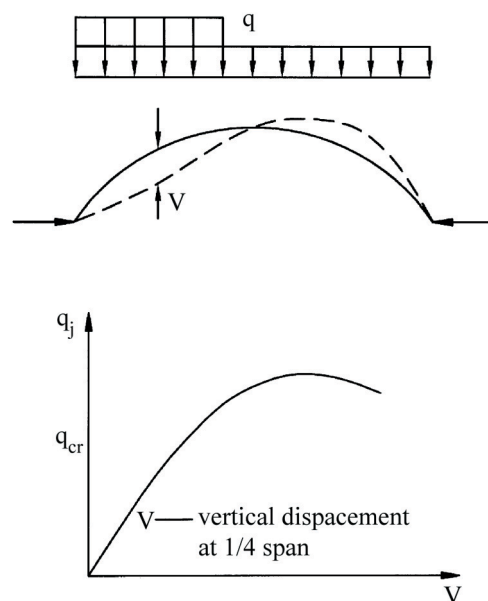


Figure 1. In-plane instability forms at critical points.

stability. Resolving the critical load for this type of stability problem requires nonlinear analysis methods.

Theoretical analysis shows [13–16] that the impact of symmetric initial bending deformation on the critical load of arch asymmetric buckling mode is very small. Consequently, when studying the in-plane buckling of arches, it can generally be assumed that arch axis line and pressure line coincide, allowing for the direct application of bifurcation point buckling theorem.

2.2 In-Plane Buckling Differential Equation of Circular Arch

As shown in the circular arch in Figure 2, only elastic compressive deformation begins to occur along axial directions under uniform radial load q . If the impact of axial deformation is ignored, then the arch axis line and the pressure line can be considered to coincide, meaning that arch is in a state of no bending moment. When the load reaches the critical value, small bending deformation v and bending moment M will occur in the arch. The buckling differential equation can be derived as following:

$$\frac{d^2v}{ds^2} + \frac{v}{R^2} = -\frac{M}{EI_x} \tag{1}$$

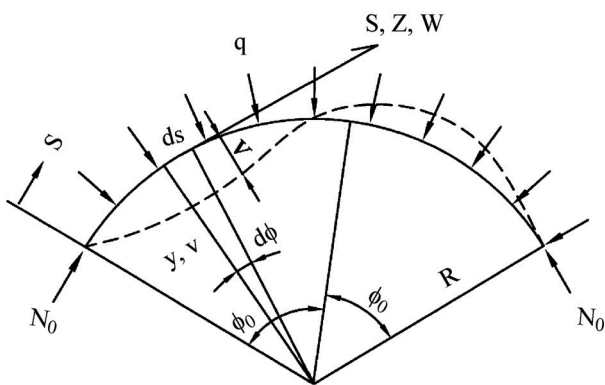


Figure 2. Circular arch under the effects of uniform radial load.

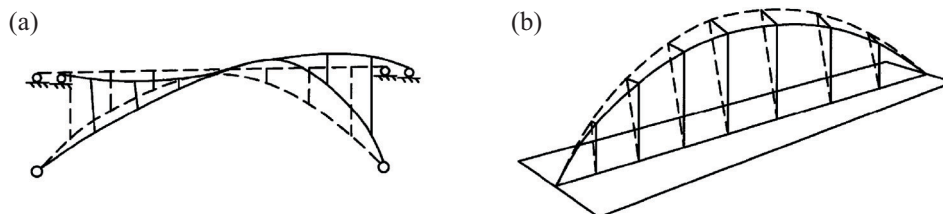


Figure 3. Effect of non-directional force on arch stability.

or

$$\frac{d^2v}{d\phi^2} + v = -\frac{MR^2}{EI_x} \tag{2}$$

In the above equations, R is the radius of circular arch; EI_x represents flexural stiffness.

2.3 Non-Directional Force of Arch Bridges

Figure 3a shows in-plane instability of a deck arch bridge. Figure 3b shows that, when a through arch tilts and becomes unstable, hangers will tilt due to the horizontal restraints applied by girders, and the horizontal component produced thereby postpones the instability occurring.

There is a common point in the above situations: the columns or hangers change their directions with structure deforming, which affects the stability of the arch. For the arch ribs, the forces exerted by the columns or hangers can be treated as external forces and their directions change with the arch ribs deforming. The forces are referred to as non-directional force. Non-directional force has positive effects on stability of through arch, but it has negative effects on stability of deck arch.

Reference [17] points out that the restrained conditions of the ends of the girder has a very large effect on the stability of deck arch bridges. As shown in Figures 4a and b, if one end of the stiffened main girder is fixed and the other is free, the critical load on the deck is about 25%~30% smaller than on the arch. If both two ends of the girder are hinges (Figures 4c, d), the magnitude of critical load is unrelated to the location of the load and is same as those of Figure 4a. The reason for this is that, for the structure shown in Figure 4b, when instability occurs in arches, the columns restrained horizontally by the girder become tilted (see dotted line in Figure 4), producing non-directional force effects and making the buckling of arch earlier.

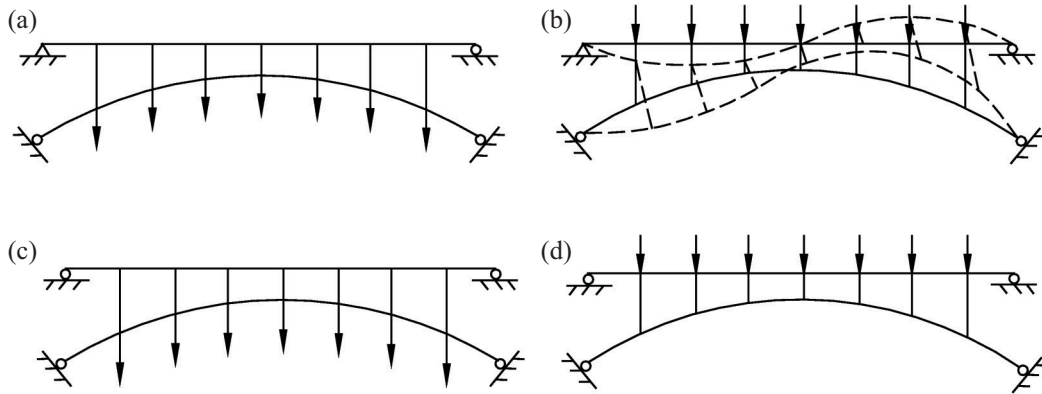


Figure 4. Effect of deck-arch bridge restraints.

3. Finite Element Analysis of Buckling of Arch Bridges

This study used RM2006 professional bridge structure analysis software developed by the Austrian company TDV GmbH to perform stability analysis for a special-shape arch bridge [18], selecting the eigenvalue method and linear elastic finite elements analysis to calculate the buckling load of the special-shape arch bridge.

Before the buckling occurring, the structure is in an initial state of linear equilibrium. Consequently, the structural incremental equilibrium equation can be expressed as [19,20]:

$$([K] + [K]_{\sigma})\{\Delta U\} = \{\Delta R\} \tag{3}$$

$[K]$ represents structural stiffness matrix, $[K]_{\sigma}$ represents structural geometric stiffness matrix, $\{\Delta U\}$ represents vector of incremental displacement, $\{\Delta R\}$ represents vector of incremental nodal force.

According to linear algebra theory, there must be:

$$|[K] + [K]_{\sigma}| = 0 \tag{4}$$

Under conditions of small deformation, $[K]_{\sigma}$ is proportional to stress. As the linear assumption is satisfied before the occurrence of buckling, stress and external load are also related in a linear manner. As a result, if the structural geometric rigidity matrix of load $\{\bar{P}\}$ is $[\bar{K}]_{\sigma}$, then the critical buckling load will be $\{P\}_{cr} = \lambda \{\bar{P}\}$ and the geometric stiffness matrix of the structure under critical load will be:

$$[K]_{\sigma} = \lambda [\bar{K}]_{\sigma} \tag{5}$$

Therefore, equation (4) can be written as:

$$|[K] + \lambda [\bar{K}]_{\sigma}| = 0 \tag{6}$$

Equation (6) is the control equation for Type 1 buckling problems. The buckling problem is converted to find the minimum eigenvalue problem of the equation.

$[K]_{\sigma}$ can be divided into the two parts of the initial internal force matrix $[K_1]_{\sigma}$ of early static loads and the initial internal force matrix $[K_2]_{\sigma}$ of later loads. When the early static load stability problem is to be considered and $[K_2]_{\sigma} = 0$, allowing for direct use of static load in calculation. Therefore, the λ calculated from equation (6) will be the stability coefficient of static load. If the buckling problem of later loads is to be considered, then static load $[K_1]_{\sigma}$ can be treated as a constant, equation (6) can thus be written as:

$$|[K] + [K_1]_{\sigma} + \lambda [K_2]_{\sigma}| = 0 \tag{7}$$

As a result, the minimum eigenvalue λ will be the safety coefficient of later load, and the corresponding eigenvector is the buckling mode.

4. Case Analysis

4.1 Basic Data for Analysis

The special-shape arch bridge studied in this paper is a steel box girder arch bridge. The main girder is a curve with radius of 600 m and span of 190 m. The arch rib with span of 180 m is skewed across the girder and its rise-span ratio is 0.3451, as shown in Figures 5a and b.

The cross section of arch rib is a single cell steel box,

7.040 m wide and 3.820 m high, as shown in Figure 5c. The cross section of main girder is also a steel box, with a girder height of 3 m, as shown in Figure 5d.

The yield strength of the steel in arch rib and main girder is $\sigma_s = 345$ Mpa, with a modulus of elasticity of $E = 2.06 \times 10^5$ Mpa, hangers are composed of high-strength parallel steel wires with ultimate strength of $\sigma_{pu} = 1670$ Mpa, the modulus of elasticity was $E = 2.0 \times 10^5$ Mpa.

4.2 Finite Element Model

The structure of this bridge consisted primarily of the main girder, arch rib, and hangers, the spatial finite elements analysis model of the bridge includes 202 nodes and 228 elements. The arch was simulated using 92 spatial beam elements, the main girder was simulated with 49 spatial beam elements, while the hangers were simulated using 28 cable elements that could only be tensioned, 28 rigid-arm elements on the arch were used to connect the upper ends of hangers with the arch. In addition, fixed constraint conditions were applied to the arch springing, vertical constraints and transversal constraints were applied to both ends of the girder; longitudinal constraint was applied to only one end.

4.3 Stability Analysis of the Original Bridge

In calculating the buckling load of this bridge, the

loads taken into account included static load, vehicle load, temperature load, and static wind load. Vehicle load was based on the Chinese common design code of highway bridge (JTG D60-2004), applying a vertical uniformly distributed load of 330 kN/m to the main girder. Temperature load was calculated in considering the worst case of overall temperature increase of 36 °C and overall temperature decrease of 41 °C. The coefficient of thermal expansion of arch rib, girder and hanger is 1.2e-5. The vertical and horizontal settlements of the arch springs are 10mm, and the vertical settlements of the girder ends are 10 mm. Static wind load was calculated by applying a 600 Pa wind load at the bridge location to the main girder and the arch. The same load conditions are used in both linear buckling analysis and geometric nonlinear buckling analysis. At the same time, to compare the non-directional force of hangers, hanger force in the completed bridge is converted to nodal concentration force acting on the bare arch rib to calculate the stability coefficient.

The above finite element model and loads were used in the buckling analysis of the original bridge. The stability coefficients obtained for the bridge under different load conditions are shown in Table 1.

Table 1 shows that, under the effects of equivalent static load on the bare arch, the stability coefficient is

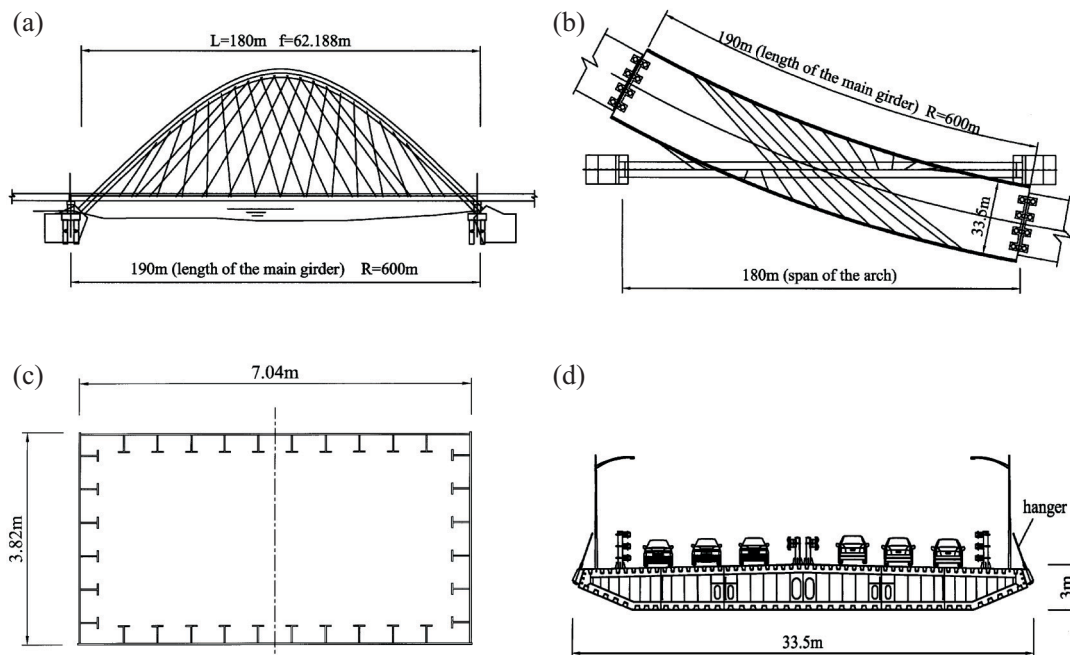


Figure 5. Drawing of special-shape arch bridge (unit: m).

12.163. Due to non-directional force effects, the stability of the overall structure is greatly increased, resulting in a stability coefficient of 20.93. The stability coefficient of linear elasticity analysis in the most disadvantageous situation is 17.491.

It can be seen from Table 1 that, under any identical conditions, the stability coefficients of linear analysis will be less than the stability coefficients of geometric nonlinear analysis. For the single arch rib, lateral force will only cause the arch to produce lateral shear force in linear analysis, in geometric nonlinear analysis, lateral force will not only cause an arch to produce lateral shear force, but also cause the arch to produce axial pull due to the impact of large deformation. Consequently, relative to linear elasticity stability analysis, due to reductions in arch axial pressure, stability coefficients taking into account geometric nonlinearity will actually be higher.

4.4 Parameter Impact Analysis

The impacts of changes in different structural design parameters on bridge stability were studied by changing structural design parameters such as height of main girder, restrained conditions of the arch, and arch vertical and lateral stiffness.

4.4.1 The Impact of the Rise-Span Ratio on the Stability Coefficient

The rise-span ratio of the original bridge was 0.345. Taking into account structural aesthetics and reasonable mechanics, the range of changes in rise-span ratio was set between 0.1 and 1.0. Stability coefficients corresponding to different rise-span ratios were calculated. Figure 6 shows the relationship between the stability coefficient and the rise-span ratio. When the rise-span ratio

is excessively large, increases of height of arch rib will lead to increases of length of arch rib, thereby reducing structural rigidity and increasing weight, finally leading to reductions of arch stability. When the rise-span ratio is excessively small, the arch will be too flat and straight. At this time the axial compression force in the arch will greatly increase, causing the arch to be more prone to destabilization. These results show that the rise-span ratio adopted by the original bridge is very reasonable.

In verification of analytical results, Li Guohao [15] once used an analytical method to determine the relationship between the stability coefficient of a parabolic arch and the rise-span ratio of a bridge, and then used experimentation to verify his results. In order to verify the accuracy of the analytical results of this study, this paper divided the stability coefficients obtained by Li Guohao and this paper by their own maximum value λ_{\max} , thereby obtaining the relationship between the ratio λ/λ_{\max} and

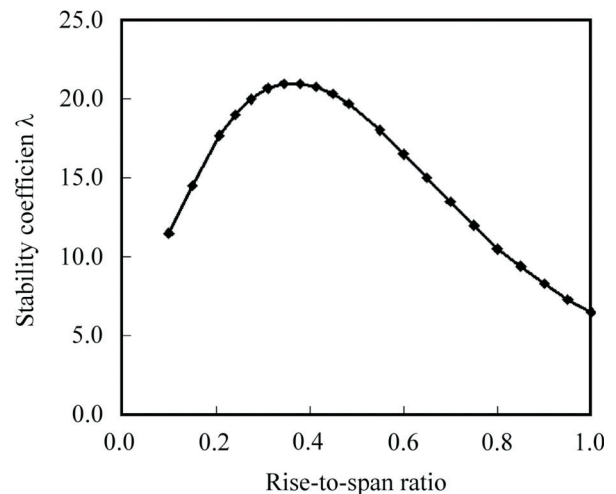


Figure 6. Comparison of stability coefficients with a change in rise span ratio.

Table 1. Results of stability analysis

Load conditions		stability coefficient (linear)	stability coefficient (geometric nonlinear)
bare arch	equivalent static load	12.163	12.174
	static load	20.930	26.719
	static load + live load	18.346	23.789
	static load + temperature increase	20.472	27.109
overall model	static load + settlement	20.796	26.914
	static load + static wind	20.379	26.328
	static load + live load + temperature increase + settlement + static wind	17.491	23.203

the rise-span ratio shown in Figure 7. This figure shows that the analytical results of this paper are very consistent with the theoretical results and experimental results in reference.

4.4.2 The Impact of Main Girder Height on the Stability Coefficient

The main girder height of the original bridge was 3 m. Table 2 gives the stability coefficients of the bridge when main girder height is 2.5 m, 3.0 m, and 3.5 m. Results demonstrate that increase of main girder height can improve the overall structural stability but that effects are limited.

4.4.3 The Impact of Restraints of Arch Springing on the Stability Coefficient

Table 3 lists the stability coefficients when the restrained conditions of arch are respectively fixed restraint, ball joints and axial joints. As can be seen, that fixed restraint of arch springing is of great help to overall structural stability. When arch springing are completely restrained, structural destabilization is in-plane buckling mode. Stability is affected by the in-plane stiffness of the

arch, if in-plane rotating restraints of arch springing are removed, in other words using axial hinge joints, then the in-plane stiffness of the arch is greatly reduced, thereby greatly reducing the stability coefficient of the structure. When out-of-plane rotating restraints of arch springing are removed, there is only a very small reduction of arch in-plane rigidity. Consequently, the stability coefficient using ball hinge joints is slightly smaller than the stability coefficient using axial hinge joints.

4.4.4 Impact of Flexural Stiffness of Arch Rib on Stability Coefficient

In order to study the impact of flexural stiffness of arch rib on the stability coefficient, the vertical moment of inertia I_y of arch rib was set at a range between 0.5 times to 2.0 times the original value, lateral moment of inertia I_z of arch rib was also set between 0.5 times to 2.0 times the original value. Figure 8(a) shows that increasing the vertical flexural stiffness of the arch can effectively increase the stability of the overall structure, as the destabilization of the arch is in-plane buckling mode, increases in vertical flexural stiffness has a significant impact on increasing the stability of the arch.

Figure 8(b) shows that increasing the lateral flexural stiffness of the arch will increase the stability of the overall structure, but the impact is very little when the lateral flexural stiffness has a large value. This is because the stability of the arch is determined by the vertical flexural stiffness of the arch. Increasing the lateral flexural stiffness does not have a significant impact on the occurrence of in-plane buckling. However, when the lateral rigidity of the arch is reduced to a certain value, out-of-plane

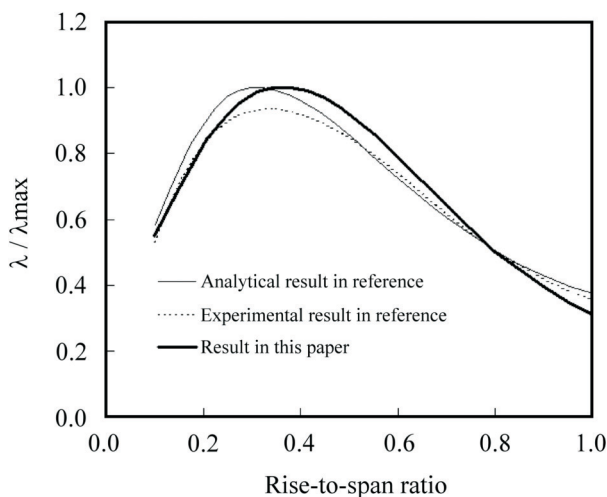


Figure 7. Comparison of stability coefficients in this paper and Reference 11.

Table 2. Impacts of girder height on stability coefficients

girder height (m)	stability coefficient
2.5	16.82
3.0	17.49
3.5	18.45

Table 3. Impacts of arch springing restraint on stability coefficients

arch springing restraint	stability coefficient
no hinge (arch springing completely fixed)	20.93
spherical hinge joint (arch springing can rotate in three directions)	9.85
axial hinge joint (arch springing can rotate along horizontal axis)	9.93

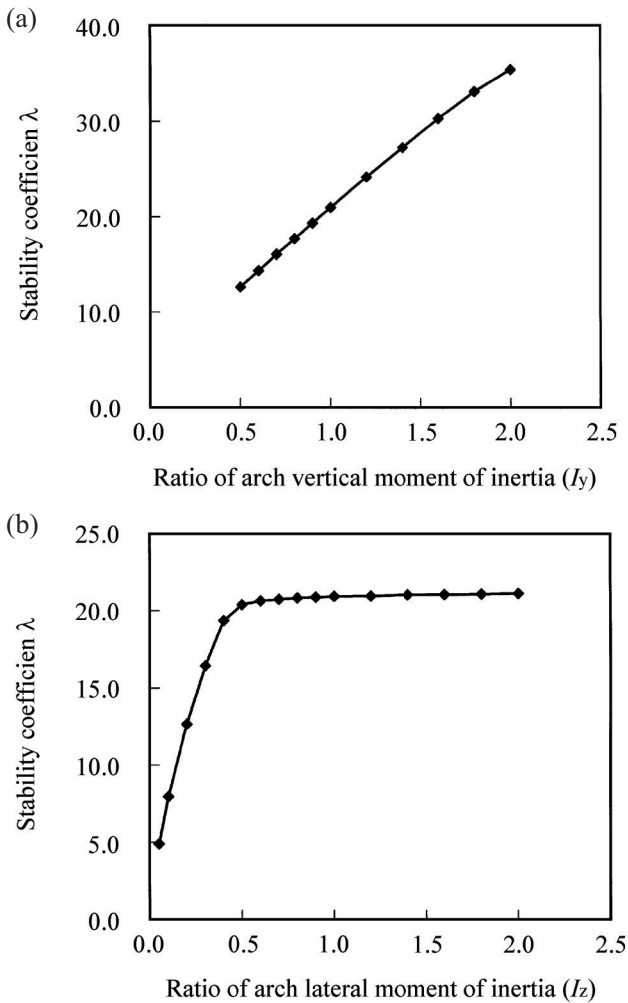


Figure 8. Comparison of stability coefficients with a change in I_y and I_z of arch.

buckling will occur before in-plane buckling due to the reduction of lateral rigidity. At this time, the stability of the arch is determined by lateral rigidity; lower lateral rigidity leads to a lower stability coefficient.

5. Conclusion

Arch bridges are a type of structure primarily intended to withstand compression force, causing studies regarding stability to be very important. Based on the buckling analysis of the overall structure, the following conclusions can be given:

(1) If a deck arch bridge tilts and becomes unstable, vertical column will tilt as a result of restraints of the girder. The horizontal component force produced thereby will accelerate the tilt of the bridge. This is a

negative effect produced by non-directional force on arch bridge stability.

- (2) Diagonally placed hangers tend to postpone the buckling of arch occurring and improve the overall structural stability. This is a positive effect provided to special-shape arch bridge stability by non-directional force.
- (3) For single arches, as large deformations will cause arch axial compression to be reduced and will also stability coefficients to be larger than the results of linear elasticity stability analysis, just performing linear elasticity stability analysis is sufficient for single arches with lateral effects.
- (4) Increasing the height of main girder is of substantial aid to overall structural stability, but the effect is limited.
- (5) The restrained conditions of arch springing influence markedly on the overall structural stability. The stability coefficients associated with use of ball joints or axial joints are similar. When complete restraint is used, the stability coefficient is more than twice the coefficients associated with ball joints or axial joints.
- (6) The rise-span ratio has a relatively large impact on overall stability. Excessively large or small rise-span ratio is disadvantageous for structural stability. The reasonable rise-span ratio for the bridge studied in this paper is around 0.37.
- (7) Increasing vertical rigidity of arch can effectively increase overall structural stability, increasing the lateral rigidity of arches can increase overall structural stability, but the impact is insignificant once a certain value is reached.

References

- [1] Timoshenko, S. and Gere, J., *Theory of Elastic Stability*, 2nd ed. New York, NY: McGraw-Hill (1961).
- [2] Ziegler, H., *Principles of Structural Stability*, Blaisdell, Waltham, MA (1968).
- [3] Austin, W.-J. and Ross, T.-J., "Elastic Buckling of Arches under Symmetrical Loading," *Journal of Structural Division. ASCE*, Vol. 102, pp. 1085–1095 (1976).
- [4] Harrison, H., "In-Plane Stability of Parabolic Arches," *Journal of Structural Division. ASCE*, Vol. 108, pp. 195–205 (1982).

- [5] Mirmiran, A. and Amde, A. M., "Inelastic Buckling of Prestressed Sandwich or Homogeneous Arches," *Journal of Structural Engineering*. ASCE, Vol. 119, pp. 2733–2743 (1993).
- [6] Pi, Y.-L. and Trahair, N.-S., "In-Plane Inelastic Buckling and Strengths of Steel Arches," *Journal of Structural Engineering*. ASCE, Vol. 122, pp. 734–747 (1996).
- [7] Arie, R. and Charalampos, B., "Investigation of the Arch In-Plane Buckling Behaviour in Arch Bridges," *Journal of Constructional Steel Research*, Vol. 64, pp. 1349–1356 (2008).
- [8] Stüssi, F., "Lateral Buckling and Vibration of Arches," *Int. Assoc. of Bridges and Structural Eng. Pubs.*, pp. 327–338 (1973).
- [9] Wen, R.-K. and Medallah, K., "Elastic Stability of Deck-Type Arch Bridges," *Journal of Structural Engineering*, ASCE, Vol. 113, pp. 757–768 (1987).
- [10] Raymond, H.-P., "Buckling of Shallow Arches with Supports that Stiffen When Compressed," *Journal of Engineering Mechanics*, Vol. 116, pp. 973–976 (1990).
- [11] Pan, S.-S., *Lateral Stability Study of Concrete-Filled Steel Tubular Narrow Arch Bridge*, PhD thesis, Dalian University of Technology (2004).
- [12] Xing, F., Zhu, B. and Wang, X.-P., "Stability Analysis for CFST Basket Handle Arch Bridge," *International Conference on Transportation Engineering*, pp. 1378–1383 (2009).
- [13] Xiang, H.-F. and Yao, L.-S., supervisor, *High-Level Bridge Structure Theory*, Beijing: China Communications Press (2001).
- [14] Dai, Z.-F., *Steel Bridges*, Beijing: China Railway Publishing House (1983).
- [15] Li, G., *Bridge Structure Stability and Vibration*, Beijing: China Railway Publishing House (2003).
- [16] Xiang, H.-F. and Liu, G.-D., *Vibration and Stability of Arch Structures*, Beijing: China Communications Press (1990).
- [17] Yang, G., *Arch Axis Optimization and Stability Analysis for Special-Shape Arch Bridges*, Dalian University of Technology Bridge Engineering Research Institute (2008).
- [18] TDV GmbH, *RM2006 Technical Description*, TDV-Austria (2006).
- [19] Stevens, L.-K., *Carrying Capacity of Mild-Steel Arches*, Proc ICE (1957).
- [20] Ronca, P. and Cohn, M.-Z., "Limit Analysis up to Concrete Arch Bridges," *ASCE*, Vol. 105 (1979).

Manuscript Received: Jun. 12, 2009

Accepted: Jan. 27, 2010